



Universidad Autónoma  
de Madrid

**Biblos-e Archivo**  
Repositorio Institucional UAM

**Repositorio Institucional de la Universidad Autónoma de Madrid**

<https://repositorio.uam.es>

Esta es la **versión de autor** del artículo publicado en:  
This is an **author produced version** of a paper published in:

Science of the Total Environment 645 (2018): 146-155

**DOI:** <https://doi.org/10.1016/j.scitotenv.2018.07.120>

**Copyright:** © 2018 Elsevier Ltd. This manuscript version is made available under the CC-BY-NC-ND 4.0 licence <http://creativecommons.org/licenses/by-nc-nd/4.0/>

El acceso a la versión del editor puede requerir la suscripción del recurso

Access to the published version may require subscription

# Stevensite-based geofilter for the retention of tetracycline from water

Raúl Fernández<sup>a,\*</sup>, Ana Isabel Ruiz<sup>a</sup>, Carlos García-Delgado<sup>b, c</sup>, Daniel González-Santamaría<sup>a</sup>, Rafael Antón-Herrero<sup>b</sup>, Felipe Yunta<sup>b</sup>, Caudia Poyo<sup>a</sup>, Andrea Hernández<sup>a</sup>, Enrique Eymar<sup>b</sup>, Jaime Cuevas<sup>a</sup>

<sup>a</sup> Department of Geology and Geochemistry, Faculty of Sciences, Autonomous University of Madrid, Cantoblanco, 28049 Madrid, Spain

<sup>b</sup> Department of Agricultural Chemistry and Food Sciences, Faculty of Sciences, Autonomous University of Madrid, Cantoblanco, 28049 Madrid, Spain

<sup>c</sup> Institute of Natural Resources and Agrobiological Sciences (IRNASA-CSIC), Cordel de Merinas 40-52, 37008 Salamanca, Spain

## Article history:

Received 30 April 2018

Received in revised form 9 July 2018

Accepted 10 July 2018

Available online xxx

## Keywords:

Tetracycline

Geofilter

Stevensite

Adsorption

Contaminated waters

## ABSTRACT

The antibiotic tetracycline, is considered a contaminant of emerging concern due to its presence in wastewater effluents, surface waters and groundwaters. Adsorption of tetracycline on soils and clays has been extensively studied to remove the contaminant from the water. A decreasing adsorption as the pH increases is normally reported in the pH range 3–9. However, adsorption isotherms performed on a commercial stevensite presented increasing adsorption with the increasing pH, in the pH range 2–8. This is very interesting since the pH in natural and wastewaters are normally in the range 6–8. A laboratory design of a geofilter using a mixture of sand and stevensite was tested against an inflow solution of tetracycline 1 g/L, NaNO<sub>3</sub> 0.1 M and pH=7 in an advective transport cell experiment. The number of tetracycline molecules exceed by >3 times the number exchangeable positions in the stevensite geofilter. Under these conditions, the TC adsorption on the geofilter reaches 590 mg/g, surpassing the retention capacity of most adsorbents found in literature. Besides, the tetracycline is completely desorbed by the inflow of a saline solution (Mg(NO<sub>3</sub>)<sub>2</sub> 0.5 M, at pH=2) with capacity to replace the exchangeable positions, thus, recovering the geofilter and the tetracycline. © 2018.

## 1. Introduction

Pharmaceuticals, and among them antibiotics, are widely consumed for human and veterinary use and released to the environment with undervalued consequences on ecosystems and water quality. The greatest concern of releasing antibiotics to aquatic environments, either directly or indirectly by surface runoff or soil leaching, is related to the evolution of antimicrobial resistance genes and antimicrobial-resistant bacteria, which reduces the therapeutic potential against human and animal pathogens (Tran et al., 2018).

Tetracycline (TC), an organic chemical compound of broad spectrum of antibiotic action, has been listed by the United States Environmental Protection Agency (USEPA) and the European Union (EU) as a contaminant of emerging concern (CECs) due to the increasing presence in surface waters, groundwaters, sea waters, drinking waters and wastewater effluents.

Tetracycline and its derivatives are usually resistant to biodegradation processes. Around 50–80% of the parental compound is found under the unmodified form in urban wastewater effluents (Michael et al., 2013) since humans and animals do not metabolize most of the ingested tetracycline and eliminate it through urine and feces (Mahamallik et al., 2015). This is why tetracycline concentrations found in waters have been increasing worldwide in the recent years. Many studies report tetracyclines concentration in raw and treated

sewage within the ng/L to µg/L range (Kim et al., 2005; Yang and Carlson, 2003). Concentrations of TC, oxytetracycline (OTC) and chlortetracycline (CTC) up to 0.1 µg/L were determined in 139 stream sites all across the United States country in the period 1999–2000 (Kolpin et al., 2002) while higher averaged concentrations, 10 µg/L of TC and 73 µg/L of OTC, were determined in wastewaters from 27 large-scale animal farms of the Jiangsu province (China) in 2009 (Wei et al., 2011). However, other studies report concentrations of TCs in the mg/L order of magnitude in wastewater outflows near pharmaceuticals and animal farms facilities (Hou et al., 2016; Li et al., 2009).

Conventional treatments used in urban wastewater plants are based on physical and chemical processes such as filtration, coagulation/flocculation and sedimentation, but most of the reduction of the organic matter relies on aerobic and anaerobic biological systems in activated sludge tanks that consumes the organic compounds. However, in those systems the antibiotics are considered toxic to the microorganisms.

Filtration through a porous media including a specific adsorbent material for antibiotics can be performed prior to the entrance of water to the plant, but the method could have several disadvantages if the contaminant is not degraded or the adsorption efficiency is low (Homem and Santos, 2011). Indeed, the adsorbed contaminant may generate a new solid waste to be managed if there is not any technical process to recover separately the contaminant and the adsorbent. As discussed by Ren et al. (2018a), carbonaceous amendments (such as activated carbon and biochar) and carbon nanomaterials, highly recommended in soil remediation to decrease the bioavailability of or-

\* Corresponding author.

Email address: raul.fernandez@uam.es (R. Fernández)

ganic pollutants, may have a potential ecological risk for the soil biota.

Carbon nanotubes and ion exchange resins have been studied to remove antibiotics from wastewater, however their high adsorption coefficients contrast with their elevated production and operational costs (Ahmed et al., 2015). Cost-effective materials, such as clays, have been studied to adsorb antibiotics (Figuerola et al., 2004). Montmorillonite, kaolinite, palygorskite, rectorite are some clay minerals that have been used for this purpose. Stevensite, a trioctahedral smectite with layer charge derived from vacant octahedral positions and characterized by large specific surface area is used in the present study.

Antón-Herrero et al. (2017) studied the adsorption capacity of TC, OTC and CTC on a commercial stevensite, demonstrating high removal capacity from solution through cation exchange displacement. In addition, other possible adsorption mechanisms have been observed, such as surface complexation by direct interaction of positively charged TC with negatively charged edge sites of the adsorbent mineral, through interaction of negatively charged TC with the hydrated cations that act as a bridge between silanol or hydroxyl groups of the mineral surface or either through hydrogen bonding (Ren et al., 2018b).

In the present study, the same stevensite studied by Antón-Herrero et al. (2017) has been used to perform the experiments of adsorption of TC from aqueous solution on the clay. The objective was to design a cost-effective filter able to efficiently adsorb the TC and desorb it in a further process to recover both, the TC and the geofilter.

## 2. Materials and methods

### 2.1. Tetracycline

Commercial tetracycline hydrochloride from Alfa Aesar (96% purity) was used to prepare a solution of 1 g/L TC in NaNO<sub>3</sub> 0.1 M at pH=7. The TC molecule consist of a chain of four cyclic 6-carbon rings and possess three ionizable functional groups: a) dimethylamino (pKa 3.3), b) phenolic diketone (pKa 7.7) and c) tricarbonylamide (pKa 9.7), that can undergo protonation or deprotonation, depending on solution pH. Thus, TC will predominate as a cation (+00) at pH below 3.3, will act as a zwitterion (+-0) in the pH range 3.3 and 7.7, as a monovalent anion (+--) in the pH range 7.7 and 9.7, as a divalent anion (0--) in the pH range 9.7 and 12, and as a trivalent anion at pH above 12 (Chang et al., 2009b; Jin et al., 2007). Under the experimental condition imposed in the present study, TC will behave as a zwitterion with capacity to adsorb in both negatively and positively charged sites.

### 2.2. Stevensite

The clay used in the present study, a raw stevensite, was supplied by Tolsa (Spain) with the commercial name of Minclear N100™. The mineralogical composition is dominated by stevensite (>90%) and accessory minerals are present (<10% illite and dolomite and <1% feldspars and quartz). Stevensite is a clay mineral from the smectite group, characterized by a 2:1 trioctahedral structure with deficiency in the total number of ions in octahedral positions that should be occupied by Mg (Faust and Murata, 1953; Güven, 1991).

### 2.3. Batch experiments

Adsorption isotherms were performed in polypropylene centrifuge tubes (batch experiments). Initial TC concentrations of 50, 100, 200,

400, 600 and 1000 mg/L were prepared in NaNO<sub>3</sub> 0.1 M in order to maintain a fix ionic strength. The suspensions included 50 mg of stevensite into a total volume of 20 ml, after the addition of a constant volume of HNO<sub>3</sub> used to fix a pH interval to ~2, ~3, 4–5 and 6–7.5. The pH increased gradually over time, therefore, some tests were performed with the objective to add a fix volume of acid and measure the desired pH after the interaction time, set to 1 h. All experiments were performed in duplicate and a blank assay, without stevensite, was performed for each series of experiments.

TC-stevensite interaction was performed in the closed centrifuge tubes inserted in a rotatory shaker, in absence of light and at constant ambient temperature (20–22 °C). Afterwards, pH was measured to control the desired pH range and the tubes were centrifuged at 10000 rpm for 5 min. Immediately, an aliquot of sample was retired from the suspension, diluted and measured by spectrophotometry at 254 nm in a Milton Roy Spectronic 1201 model spectrometer. The experimental isotherms data were fitted to Langmuir and Freundlich theoretical models according to the following equations:

$$\text{Langmuir model : } S = \frac{S_m K_L C}{1 + (K_L C)}$$

where  $S$  is the amount of TC sorbed on stevensite at equilibrium (mg/g),  $S_m$  is the maximum adsorption capacity (mg/g),  $K_L$  is the Langmuir coefficient (L/mg) and  $C$  is the equilibrium TC concentration (mg/L).

$$\text{Freundlich model : } S = K_f C^n$$

where, in addition to  $S$  and  $C$  as defined for the Langmuir model,  $K_f$  is the Freundlich constant (L/g) and  $n$  is the Freundlich exponent (an empirical parameter usually <1) that account for the sorption intensity.

The term  $S$  was calculated by the mass balance equation

$$\begin{aligned} &: S \\ &= \frac{(C_0 - C) V}{m} \end{aligned}$$

where  $C_0$  is the initial TC concentration (mg/L),  $V$  is the volume of solution (l) and  $m$  is the mass of the dry stevensite clay (g).

The software Microsoft Excel Spreadsheets for Fitting Sorption Data (Bolster and Hornberger, 2007) was used for the fitting of the adsorption isotherms.

### 2.4. Transport experiments

The experimental design of the transport experiments in cylindrical columns is composed by a mixture of silica sand and stevensite in mass ratio 10:1. Silica sand was finely grinded in order to obtain a compacted mixture where stevensite is trapped within the mixture. The sand-stevensite mixture, filters, o-rings and porous filling materials were inserted into the methacrylate columns in the following order from bottom to top: 1) a polypropylene filter of 0.45 µm pore size, 2) a polypropylene geotextile filter disk, 3) glass or silica sand, 4) a porous Teflon disk, 5) a stainless steel sintered filter with Viton® o-ring on top and bottom, 6) the sand-stevensite mixture. Then, the inverse order of materials was used to complete the filling of the column. Three replicates experiments were run using 20 g of mixture

(18 g of silica sand and 2 g of stevensite) A blank experiment, using the same experimental design but excluding the stevensite clay, was performed in order to verify that filters, sand or even the methacrylate material used in the column did not adsorb TC and, hence, all TC adsorption must be attributed to stevensite.

An additional shorter time experiment was performed using 5 g of mixture with the same mass ratio in order to include a desorption process in a second step using a  $\text{Mg}(\text{NO}_3)_2$  0.5 M solution at pH=2. For the latter experiment a similar design was used, replacing the glass sand by silica sand and using another design of cylindrical column. Stainless steel sintered filters were not used due to volume impediment. In any case, these minor changes had no impact on the results. The main objective of filters and filling material is to maintain in site the stevensite clay that, due to its small particle size, could advectively be displaced from the geofilter design to the outflow. A constant flow rate of 2 mL per minute was applied from the TC solution tank through a piston pump that injected the solution from the bottom side into the column. At the upper side, the outflow solution was collected in syringes. A switch device before the syringes permitted to collect alternatively the solution in two sequential syringes maintaining the constant flow and without any loss of fluid. Every syringe was filled up to an approximate volume of 5 ml. The exact volume was calculated by mass weight of syringes containing the outflow solution and assuming a fluid density equal to 1 g/mL. A scheme of the experimental design and photographs of the both types of columns are presented in Fig. 1. The change in the design of the cylindrical columns was performed to prevent from aqueous leakages originated in the threads after intensive use, although that problem did not happen in the present work.

Assuming a mineral density of  $2.65 \text{ g/cm}^3$  for the sand-stevensite mixture and considering the dimensions of the cylindrical transport cells (height of 1.4 and 0.5 cm in columns b and c of Fig. 1 and 1.5 cm of radius in both columns), a pore volume of 2.35 and  $1.65 \text{ cm}^3$  is obtained for each column.

## 2.5. Analytical methods

The Milton Roy Spectronic 1201 model spectrometer was used to measure the absorbance of TC in batch experiments and in the adsorption/desorption transport experiment. TC concentrations were calculated by means of a calibration line of best fit.

The TC concentration in the three replicates transport experiment was measured by high performance liquid chromatography (HPLC) analysis using the same methodology and equipment as in Antón-

Herrero et al. (2017). The HPLC equipment is composed of a separation module (2695 Waters, Milford, MA) equipped with an Agilent ZORBAX SB-C8 separation column ( $250 \times 4.6 \text{ mm}$ ,  $5 \mu\text{m}$  particle size) and photodiode array detector (Waters 996 PDA). TC chromatograms are quantified at 355 nm.

Mineralogical characteristics (X-ray diffraction) and physico-chemical properties (specific surface area and cation exchange capacity) of the sand-stevensite mixture solid samples were determined before and after the transport experiments.

X-ray diffraction (XRD) was performed on randomly oriented dried powder and oriented  $<2 \mu\text{m}$  size fraction. The diffractometer used was an X-PERT Panalytical instrument with an X-CELERATOR detector. Measurements were taken at  $0.016^\circ$   $2\theta$  angular steps for a time of exposure of 100 s per step. The equipment uses monochromatic radiation provided by a Ge 111 monochromator. The software X'Pert Highscore was used for data treatment and identification of mineral phases.

The specific surface area of the solid silica sand-raw stevensite mixture was measured using the BET-method (Brunauer, Emmett and Teller) by  $\text{N}_2$  adsorption with a Gemini V analyzer from Micromeritics™.

The cation exchange capacity (CEC) of the silica sand-raw stevensite mixture was determined by the method proposed by Meier and Kahr (1999) using a solution of  $\text{Cu}(\text{II})$ -triethylenetetramine.

Additionally, Infrared (IR) spectral measurements and oriented aggregates (with and without ethylene-glycol) for XRD determination were performed on TC-stevensite aqueous suspensions in order to improve the structural interpretation of the TC interaction with the stevensite. The suspensions were prepared by the addition of a fix amount of stevensite (1 g) to TC solutions of 0.1 and 0.3 g/L. Both solutions were buffered to pH 7. Analytical IR determinations were performed using a PerkinElmer Spectrum Two spectrometer within the mid-IR ( $4000\text{--}450 \text{ cm}^{-1}$  wavenumber) range. All spectra of the samples in KBr pellets (1% w/w) were recorded with a  $4 \text{ cm}^{-1}$  resolution and 10 scans.

Two aliquots of the suspensions were smeared in glass slides in order to obtain oriented aggregates for XRD measurement of the basal spacing of the 2:1 sheet silicate smectitic material (Moore and Reynolds, 1997). Two other aliquots were mixed with liquid ethylene-glycol (EG) at a ratio of 1:1 wt%.

## 2.6. Transport models

Two simulations, a direct and an inverse transport model, have been performed to reproduce the short-time adsorption transport experiment.

The direct model makes use of the general transport equation for porous media (Appelo and Postma, 2005), expressed as:

$$C_e(T) = \frac{1}{2} \text{erfc} \left[ \left( \frac{P}{4 \times R \times T} \right)^{\frac{1}{2}} \times (R - T) \right]$$

where  $C_e = \frac{C_i}{C_0}$  is the relative concentration (in the range 0–1),  $T$  is the number of pore volumes,  $\text{erfc}$  is a mathematical function known as the complementary error function,  $R$  is the retardation factor that quantify the retardation between a solute (TC in the present study) due to sorption processes on transport compared to water migration and  $P$  is the Péclet number (a measure inversely proportional to the degree of dispersion experienced by a solute). All the parameters included in the equation are dimensionless.

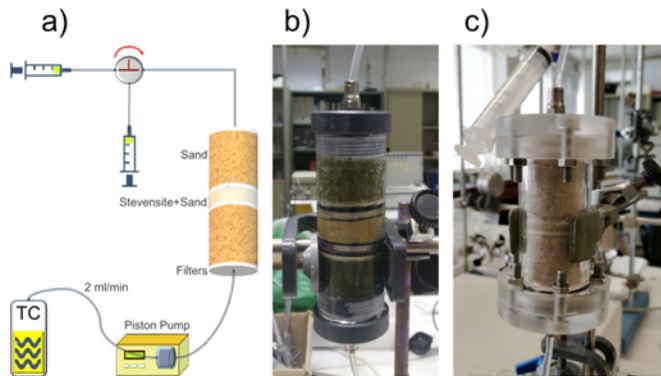


**Fig. 1.** Transport experiment in cylindrical columns: a) experimental design of the system, b) column prepared for the three replicates experiment and c) column prepared for the adsorption-desorption experiment.

$R$  is calculated by the expression:

$$R = 1 + \left( \frac{\rho_b}{\theta} \times K_d \right)$$

where  $\rho_b$  is the apparent density (g/cm<sup>3</sup>),  $\theta$  is the porosity (–) and  $K_d$  is the distribution coefficient obtained experimentally by the batch experiments.

$P$  is calculated by the expression:

$$P = \frac{q \times L}{A \times D}$$

where  $q$  is the discharge (cm<sup>3</sup>/s),  $L$  is the length of the column (cm),  $A$  is the cross-sectional area (cm<sup>2</sup>) and  $D$  is the dispersion coefficient (cm<sup>2</sup>/s), which is the only unknown parameter, used as a fitting variable to solve the transport equation.

The inverse transport model was performed with the code STANMOD (van Genuchten et al., 2012) in order to analyze the experimental breakthrough curve (BTC). Several authors obtained good results for the analysis of the performance of filter columns employing the inverse option problem of the two-site deterministic non-equilibrium convection-dispersion equation (CDE) with the CXTFIT module (Miralles et al., 2010; Nir et al., 2012; Toride et al., 1995). The CXTFIT and the STANMOD algorithms have been widely employed for the analysis of solute transport accompanied by adsorption processes. The filter is taken as a fixed-bed column and was treated as a whole 8.5 cm length and 3 cm diameter cylinder. The two-site sorption concept presumes that sorption or exchange sites can be classified into two fractions: one instantaneous (exchange equilibrium) and the other considered to be time dependent. According to van Genuchten and Wagenet (1989), in a dimensionless form, the CDE equation can be reduced and solved by Laplace transforms for adsorbed solute concentrations in the two defined sites for adsorption:

$$\begin{aligned} (1) : & \beta \times R \times \left( \frac{\partial C_1}{\partial T} \right) \\ &= \left[ \frac{1}{P} \times \left( \frac{\partial^2 C_1}{\partial X^2} \right) \right] - \left( \frac{\partial C_1}{\partial X} \right) \\ &\quad - [\Omega \times (C_1 - C_2)] - (\xi \times C_1) \end{aligned}$$

$$\begin{aligned} (2) : & (1 - \beta) \times R \times \left( \frac{\partial^2 C_2}{\partial T} \right) \\ &= \Omega \times (C_1 - C_2) - (\eta \times C_2) \end{aligned}$$

where  $C_1$  and  $C_2$  (g/L) relates to the equilibrium and non-equilibrium concentration of the solutes, respectively;  $T$  (also referred to as pore volume) is the dimensionless time ( $\frac{vL}{Q}$ ), being  $L$  the column length,  $t$  the time and  $v$  the average porewater velocity (water flux divided by the water content);  $X$  is the dimensionless distance ( $\frac{x}{L}$ );  $P$  and  $R$  are the Péclet number and the retardation factor previously defined;  $\beta$  is the fraction of equilibrium solute retardation (mobile/immobile), defined as:

$$\beta = \frac{\theta + (F \times \rho_b \times K_d)}{\theta + (\rho_b \times K_d)}$$

where  $F$  is the fraction of sites available for instantaneous sorption;  $\Omega$  is a dimensionless mass transfer coefficient, defined as:

$$\Omega = \frac{\alpha \times (1 - \beta) \times R \times L}{v}$$

where  $\alpha$  is a first order rate coefficient for kinetic sorption;  $\xi$  and  $\eta$  are coefficients depending on first order decay reaction rates accounting for solute degradation in liquid ( $\mu_1$ ) and solid ( $\mu_2$ ) sites.

The CXTFIT code fits the BTC with  $v$ ,  $D$ ,  $R$ ,  $\beta$ ,  $\Omega$ ,  $\mu_1$  and  $\mu_2$  as adjustable parameters. The fitting was performed by fixing  $v$  ( $1.88 \times 10^{-2}$  cm/s) and  $D$  ( $1.05 \times 10^{-6}$  m<sup>2</sup>/s) and letting the remaining parameters to fit by the code.  $D$  and  $v$  were calculated assuming a porosity of 0.5 and a dispersivity ( $\lambda$ ) of 0.5 cm. The dispersion coefficient ( $D$ ) was calculated in this case as:

$$D = D_{lh} = \lambda \times v = \lambda \times \left( \frac{K}{\theta} \right)$$

where  $D_{lh}$  is the hydrodynamic dispersion and  $K$  is the Darcy permeability coefficient. Scale units for calculations were given in cm, minutes and g/L. The model reproduces the BTC by iterative calculations using the mode of flux average concentration.

### 3. Results and discussion

#### 3.1. Adsorption isotherms

In contrast to previous experiments of TC adsorption in clays, the adsorption isotherms of TC onto the raw stevensite clay show an increasing adsorption as the pH increases. It has been reported that TC adsorption on clays occurs mainly due to cation exchange and on external surfaces rather than due to complexation. Under acidic conditions, the cation species of TC (TC<sup>+</sup>) adsorb in clays via displacement of exchangeable cations. For instance, Li et al. (2010) reported that 4/5 of TC adsorption on a kaolinite occurred via TC<sup>+</sup> while the remaining adsorption occurred by the zwitterionic species TC<sup>0</sup>, possibly via hydrogen bonding. In smectites, TC can intercalate in the interlayer space, as observed by XRD due to the increase in the basal spacing from 12.6 to 19.5 Å (Aristilde et al., 2010; Parolo et al., 2008). However, the observed experimental results in this study showed an opposite trend to previous studies of TC adsorption on clays (Chang et al., 2009a). The experimental results of the adsorption isotherms are shown in Fig. 2, fitted to the Langmuir (a) and the Freundlich models (b). The Langmuir and Freundlich fitting parameters are presented in Table 1. The decreasing Langmuir coefficient as pH increases indicates that less fraction of stevensite surface is covered by TC, so the affinity between TC and the clay is lower at higher pH, but more adsorption happens, in agreement with the increasing maximum adsorption capacity.

The maximum adsorption capacity obtained within the pH range 6–7.5 (701 mg/g) exceed most of the values found in literature for TC on other adsorbent materials. Maximum adsorption of TC in that pH range can reach 133 mg/g on a montmorillonite (Parolo et al., 2008) and even 312 mg/g on an activated carbon derived from tyre pyrolysis

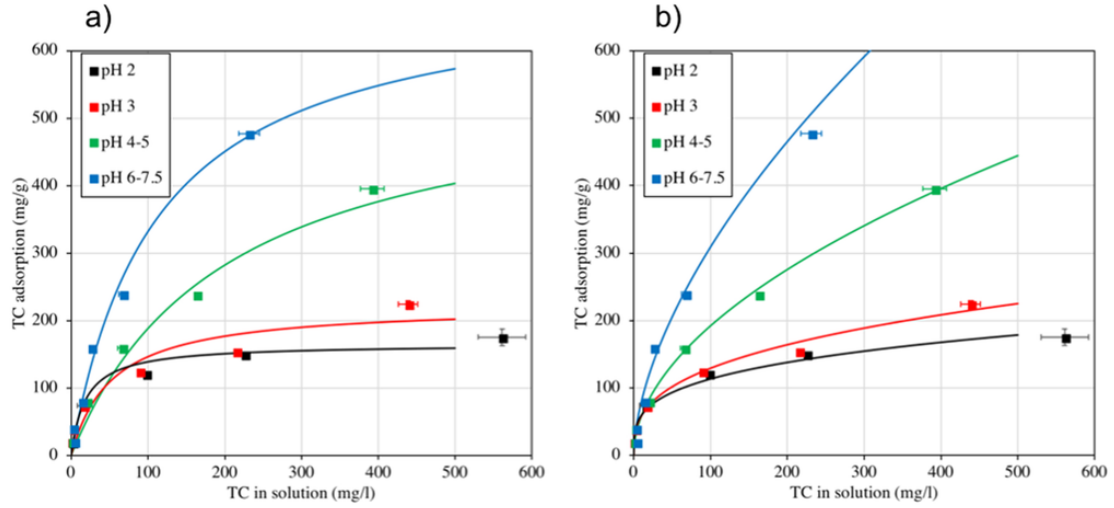


Fig. 2. Adsorption isotherms for tetracycline onto raw stevensite clay as a function of pH. a) Langmuir fitting and b) Freundlich fitting.

**Table 1**  
Fitting parameters obtained for the Langmuir and Freundlich models.

pH	Langmuir			Freundlich		
	$S_m$ (mg/g)	$K_L$ (L/mg)	$r^2$	$K_f$ (L/g)	$n$	$r^2$
6–7.5	700.6	9	0.98	20.31	0.591	0.99
4–5	564.5	5	0.97	17.44	0.521	0.99
3	223.4	19	0.89	26.39	0.345	0.97
2	165.1	53	0.95	30.96	0.282	0.97

char (Acosta et al., 2016). However, a direct comparison of  $S_m$  is not straightforward due to the dependency of experimental conditions such as temperature, solid:solution ratios, solute and adsorbent concentrations and nature, liquid phase viscosity, redox conditions, light and pH (Clive, 1968).

The Freundlich equation results into a better regression fitting, compared to the Langmuir model fitting. Increasing sorption intensity as pH increases is associated to a more homogeneous adsorption.

### 3.2. Column experiments

A blank experiment performed only with silica sand in a column presented no adsorption of TC. The high number of pore volumes required to obtain a relative concentration near to 1 is explained by the large porosity initially occupied by the filling material (glass sand), filters and tubes. The column is first saturated in deionized water and then water is replaced by the inflow TC solution at 1 g/L. Relative concentration (TC concentration determined in the outflow solution divided by the constant inflow TC concentration, 1 g/L) increases almost linearly indicating that no adsorption processes have been participated (Fig. 3). The null capacity of sand to adsorb TC in a flow-

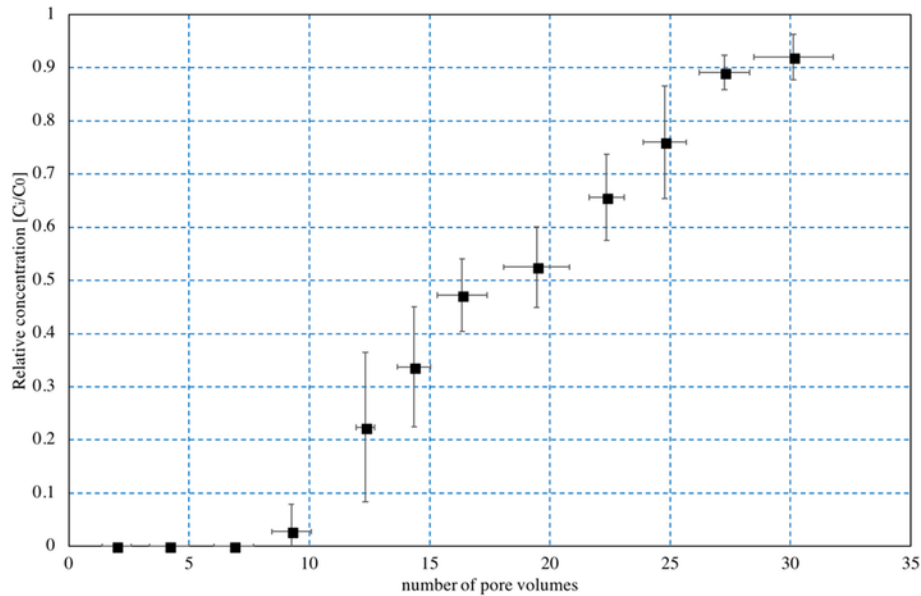


Fig. 3. Tetracycline, expressed as relative concentration, as a function of number of pore volumes in a transport blank experiment without stevensite.

through porous system was already demonstrated by Cheng et al. (2016).

Once probed that the system itself does not adsorb TC, a system with three parallel columns was run. TC concentrations were determined by HPLC.

The three replicates experiment in advective transport columns lasted approximately 5 days, although after two and a half days (~270 pore volumes) the tetracycline outflow samples were collected in large volumes and concentrations decreased. A large dispersity of data is observed over the three replicates. TC concentration measured in the outflow solution was significantly higher in one of the columns compared to the other two columns over the first ~120 pore volumes most plausibly due to the creation of preferential pathways where the TC solution could advectively move with less interaction with stevensite. Fig. 4 shows the averaged data of relative concentration of TC determined out of the column as a function of the number of pore volumes, including the calculated standard deviation after grouping all the data and presenting an averaged value for every group of five measurements. In addition, the evolution in relative TC concentration of one of the experiments with few dispersions of data is show in Fig. 4.

It can be inferred from Fig. 4 that the TC is almost completely retained over the first 50 pore volumes, then the TC concentration increases with an increasing slope that reach a maximum in the range 70–120 pore volumes, and finally the curve reaches a plateau near the relative concentration range of 0.6 in the pore volumes interval 200–250. The experiment was continued but after 250 pore volumes the lower quality of data due to TC degradation does not permit to extract further conclusions.

In any case, at 250 pore volumes a total mass of 587 mg of TC has moved through the geofilter system, meaning that the number of TC molecules has exceed the cation exchange capacity of the stevensite clay by 1.1, which is often considered the dominant mechanism to adsorb TC in clays, and still near 40% of the infiltrated TC is retained in the column.

An additional transport experiment was performed using again 1 g/L of TC and only 5 g of silica sand-stevensite clay mixture, four times less than in the three replicates experiments, in order to perform a shorter time experiment to include a desorption process in a second step (Fig. 5). The adsorption experiment lasted around 4 h at a flow rate of 2 mL per minute and was performed without any replicates, but a very similar shape of the relative TC concentration curve against number of pore volumes was obtained. A plateau is achieved when the TC relative concentration reaches 0.6. In this case, the number of TC molecules exceeding the cation exchange capacity of the stevensite clay is 3.6. A simple mass balance calculation based on the total amount of TC collected in syringes out of the column indicates that 590 mg of TC are adsorbed per gram of stevensite in the advective flow system.

Desorption with a  $\text{Mg}(\text{NO}_3)_2$  0.5 M solution at pH=2 was performed with the objective to displace by cation exchange TC adsorbed in stevensite. Surprisingly, most of the TC was displaced rapidly over the few first number of pore volumes. A maximum peak of TC concentration after only 30 pore volumes reached >5 g/L, and most of the TC was displaced after only 100 pore volumes.

The present results indicate that cation exchange is not enough to adsorb all the TC in the stevensite geofilter at near neutral pH. The desorption process required only 20 pore volumes to pass through the column an amount of  $\text{Mg}^{2+}$  equivalent to the cation exchange capacity of the stevensite clay. Therefore, the column was regenerated with all exchangeable positions occupied by  $\text{Mg}^{2+}$ . That fast replacement in exchangeable positions associated to the displacement of 3.6 times the number of TC molecules available by cation exchange suggest that an additional adsorption mechanism must take place. Antón-Herrero et al. (2017) reported the role of amide group in TC adsorption on stevensite. Other works demonstrated additional mechanisms of TC adsorption on different clays such as montmorillonite and kaolinite (Zhao et al., 2012; Zhao et al., 2015) and the important role of divalent metal cations to enhance the tetracyclines adsorption capacity of smectites (Aristilde et al., 2016).

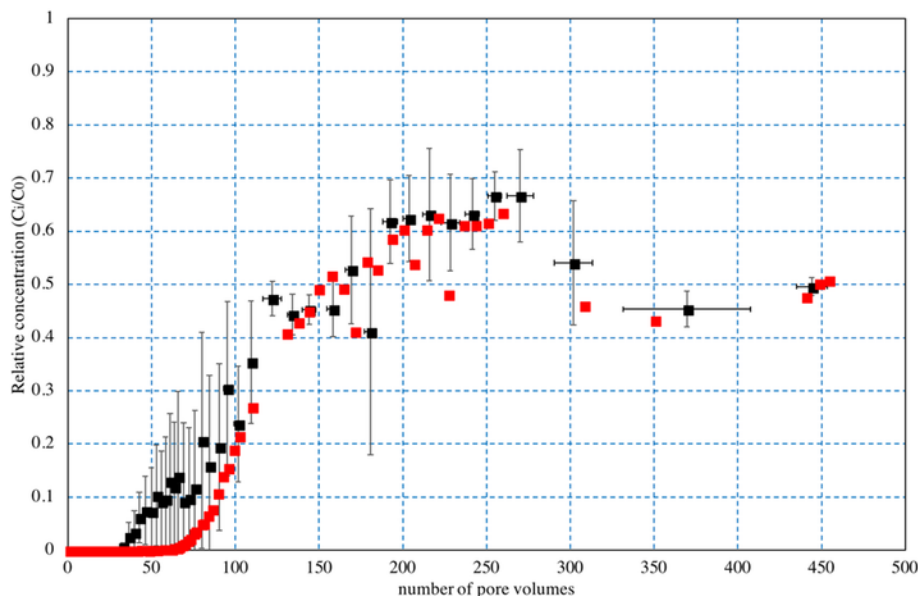


**Fig. 4.** Averaged data with standard deviations of breakthrough curves of tetracycline adsorption by stevensite for the three replicates transport experiments (black) and experimental data of one single experiment (red). Fixed concentration of the inflow TC solution is 1 g/L. A pore volume corresponds to 2.35 mL. (For interpretation of the references to color in this figure legend, the reader is referred to the web version of this article.)



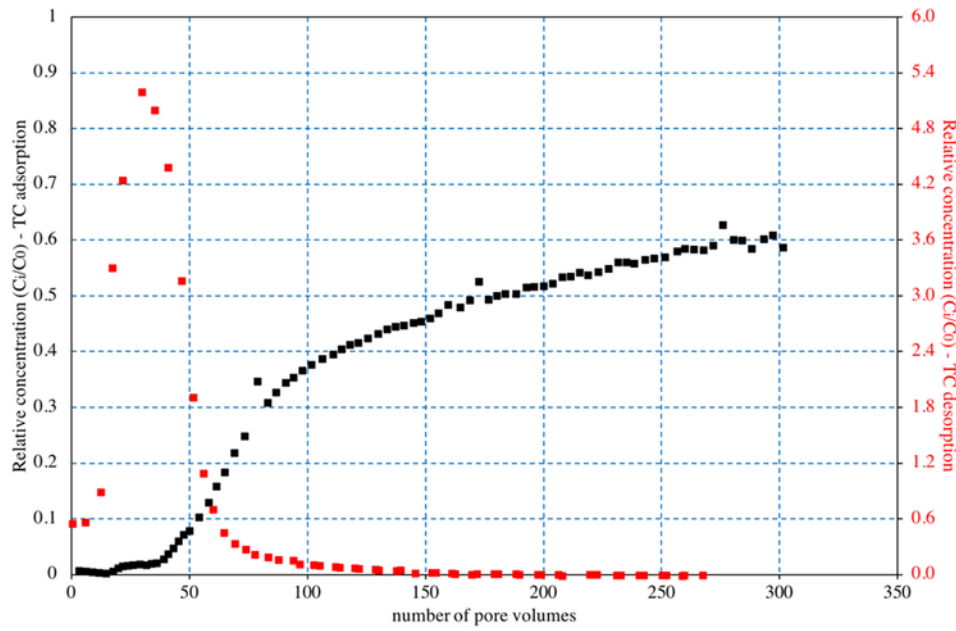


**Fig. 5.** Adsorption (black) and desorption (red) of tetracycline by stevensite in an advective flow-through system. Relative TC concentration of the adsorption process is referenced to the left Y-axis and the desorption process to the right Y-axis. Fixed concentration of the inflow TC solution is 1 g/L. A pore volume corresponds to 1.65 mL. (For interpretation of the references to color in this figure legend, the reader is referred to the web version of this article.)

### 3.3. Transport models

The value of the distribution coefficient used in the direct model (5624 L/kg) was calculated considering the batch experiments of 400 mg/L of initial concentration of the TC solution at pH in the range 6–7.5 and the concentration determined in solution once reached the equilibrium (26.56 mg/L). The calculated distribution coefficient is in agreement with other values reported in literature, which are in a wide range of  $10^2$ – $10^4$  L/kg for various sediments, clay minerals, sewage sludge and biosolids (Kang et al., 2012; Tran et al., 2018). A high retardation factor (175.5) was obtained, indicating a large sorption of TC by the sand-stevensite mixture in the column. The dispersion coefficient was fitted to  $3.2 \times 10^{-7}$  m<sup>2</sup>/s and, therefore, a value of 0.77 was obtained for the Péclet number, indicating large dispersion in the porous media compared to the solution velocity and justified by the large volume occupied in the column by the silica sand beds and filters on top and below the sand-stevensite mixture.

The mathematical function of the transport equation reproduces faithfully the behavior of the TC relative concentration as a function of the number of pore volumes (Fig. 6) for pore volumes higher than 80 and predicts the future behavior of the transport experiment. In the initial stage, at low number of pore volumes, the mathematical function does not fit correctly the experimental data due, mainly, to the large dispersion generated by those high porous inert materials previously mentioned (silica sand beds and filters).

The inverse model with STANMOD had the objective to estimate the transport parameters. The adjusted parameters are listed in Table 2. Degradation in the solid phase was fitted to be very low and can be neglected. On the other hand,  $D$  was estimated to be very close to the initial given value and is in the same order of magnitude as the value used to fit the direct model. The experimental BTC and model fitting are shown in Fig. 7 (see that the inverse model has been calculated as a function of time). The inverse model presents an excellent agree-

ment with the experimental data and support the values of the calculated parameters presented in Table 2.

### 3.4. Solid characterization

Specific surface area BET was measured on dry silica sand-stevensite clay mixtures before and after the flow-through experiments. The surface area decreases from  $19.5 \pm 3.8$  to  $6.1 \pm 0.3$  m<sup>2</sup>/g. A process of disordered aggregation in the smectite layered structures and pores occlusion is suggested for the interpretation of these data since the constancy of CEC and minor changes in random powder XRD after the transport tests may indicate that no mineralogical alteration have occurred in the experiment, except for changes in the layering order of the smectite.

The CEC determined in the mixture before and after the flow-through experiment remained constant at  $6.2 \pm 0.6$  cmol(+)/kg. It must be noted that all of the CEC in the mixture is attributed to the stevensite, which contribution in mass is only 10%. Therefore, the CEC of the stevensite clay is 10 times higher and the contribution of the silica sand is negligible or none. As the CEC in the mixture remains constant over adsorption/desorption processes a calculated mass balance, based on the charge of the displacing species, can be performed to recover the geofilter after each cycle of use.

XRD on randomly oriented powder samples suggests that there are no transformations after the experiments. Qualitative analysis displays quartz and feldspar phases and footprints of a trioctahedral smectite as the only minerals present in the mixture. Fig. 8 shows a comparison of the XRD patterns performed on oriented aggregates of the extracted <2 µm size fraction. The natural stevensite presents a basal d-spacing at 15 Å, which corresponds to divalent exchangeable cations, and the sample after adsorption (TC-stevensite) presents absence of the (001) reflection. A reflection at 10 Å, normally attributed to illite, is predominant after adsorption, but not in the original sample. This effect, although not yet understood, may reflect a microstructural change in layering stacking due to TC multi-adsorption. Fig. 8 is representative of the three replicates samples.



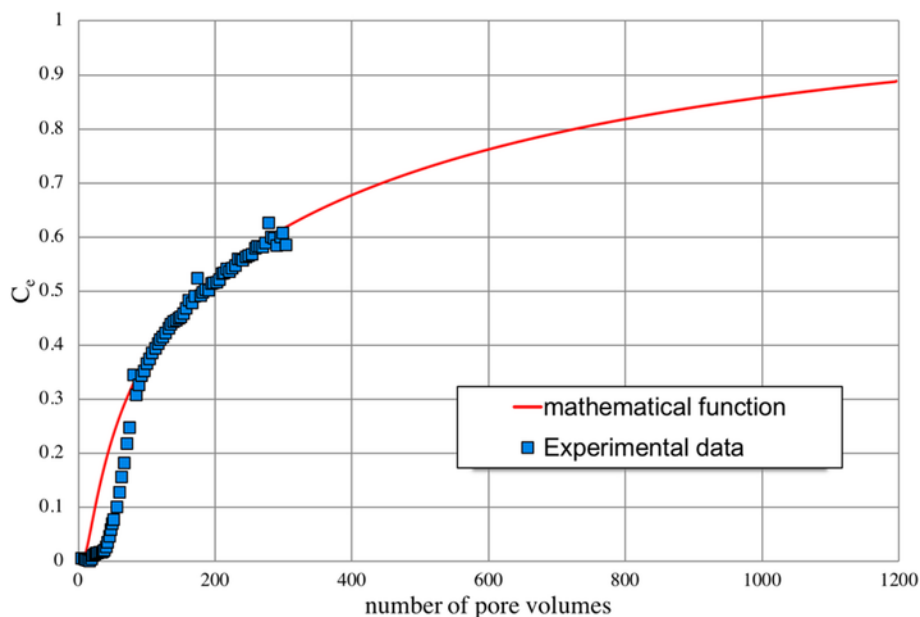


**Fig. 6.** Experimental data of tetracycline adsorption onto stevensite, expressed in relative concentration in the experimental advective flow-through system (blue squares) and mathematical curve fitting obtained by the transport equation in porous media (red line). (For interpretation of the references to color in this figure legend, the reader is referred to the web version of this article.)

**Table 2**

Two-site deterministic non-equilibrium CDE inverse model CXTFIT (Toride et al., 1995) parameters estimation within 95% confident limit (*t*-test). See the Transport models section for parameters explanation.

Parameter	Value	Standard error ( $\pm$ )
$v$ (cm/min)	1.1	–
$D$ (cm <sup>2</sup> /min)	5.7E-01	8.6E-02
$R$	2.1E+01	4.6E+00
$\beta$	3.8E-01	7.2E-02
$\Omega$	9.8E-02	6.0E-03
$\mu_1$ (min <sup>-1</sup> )	3.3E-02	1.1E-02

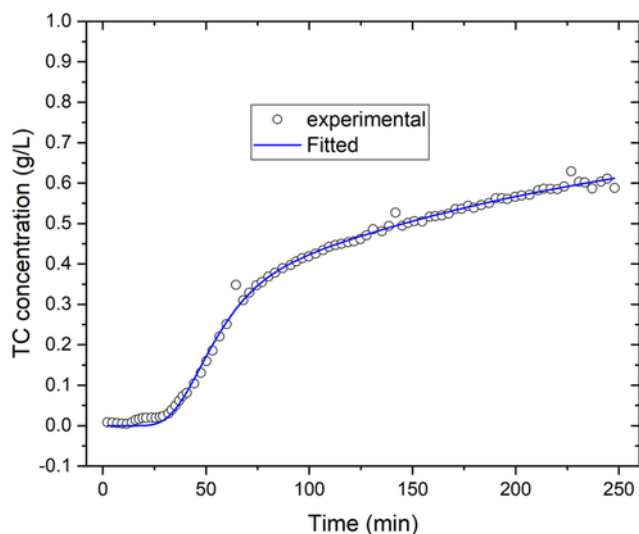


**Fig. 7.** CXTFIT fitting of the BTC of TC adsorption in the column experiment (estimated parameters are given in Table 2) using the STANMOD software (van Genuchten et al., 2012). Experimental data are shown in circles and the fitted BTC by the black line.

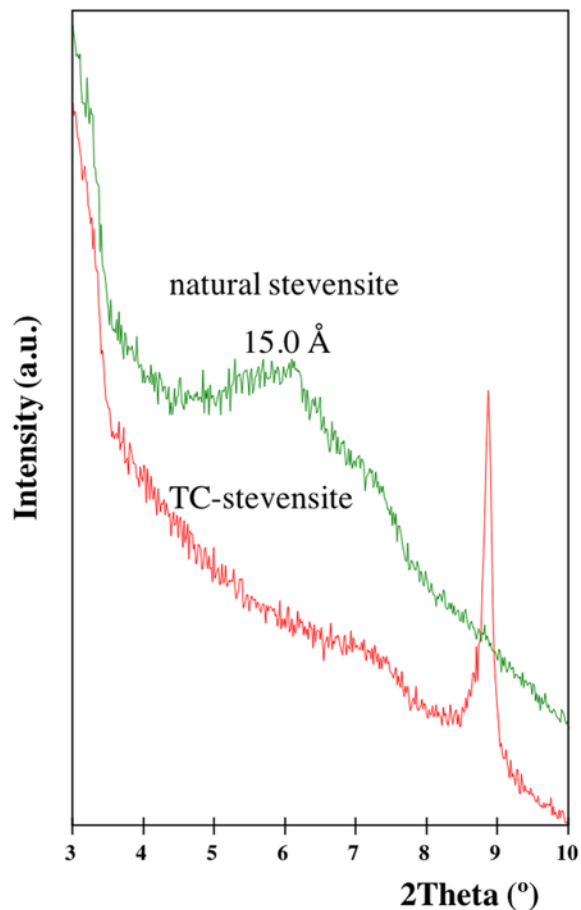


**Fig. 8.** XRD on oriented aggregate patterns of natural stevensite (green) and stevensite with adsorbed tetracycline (red). (For interpretation of the references to color in this figure legend, the reader is referred to the web version of this article.)

The disappearance of the TC-stevensite basal reflection in XRD, and the TC adsorption exceeding the stevensite CEC cannot be explained by the reported mechanisms of TC intercalation in the interlayer space of the clay minerals available in literature except, perhaps, by the exfoliation of the clay at pH 7 suggested by Chang et al. (2015) for a trioctahedral smectite under weak alkaline conditions.

This delamination could be explained by the formation of complex structures of divalent cations ( $Mg^{2+}$  and  $Ca^{2+}$ ) in the binding process with tetracyclines which have been already described by other authors (Jin et al., 2007; Othersen et al., 2003; Wessels et al., 1998). Although a variety of characterization techniques have been used to study the complexation behavior of TC, the results obtained have led to partly contrary assignments of the chelation sites as well as, stoichiometries of 1:1, 1:2, and 2:1 ions bound per tetracycline in aqueous solutions at pH in the range 6.5–8.5.

The XRD patterns of the original stevensite (Stv), samples after reaction with TC (suspensions of 0.1 and 0.3 g of TC per g of stevensite) and EG treated samples were compared (Fig. 9). As expected, natural stevensite presents an expansion of the 001 reflection from 15 to approximately 17 Å on ethylene glycol solvation. No expansion is observed on the sample with EG at the ratio of 0.3 g of TC per g of stevensite compared to the non-EG treated sample, suggesting that the interlayer cations are completely solvated by TC and it is not possible to produce the EG solvation of the stevensite. An intermediate situation is observed in samples treated with 0.1 g of TC per g of stevensite. Poorly ordered structures with a high degree of non-pillar-

ing are observed by the broad reflections at lower angles. The cations solvation is due to both, TC and ethylene-glycol.

The FTIR spectra in the band range 1200–1700  $cm^{-1}$  of the original stevensite and after interaction with TC by means of the suspension tests are shown in Fig. 10. Only this range is displayed because the most characteristic bands of TC are in this region and the bands in a wider range (400–4000  $cm^{-1}$ ) corresponding to the smectite are almost identical to the published data for standard clays (Madejová and Komadel, 2001), indicating that the adsorbed TC did not alter the stevensite structure. The bands associated with C=O stretching in TC rings (1616 and 1580  $cm^{-1}$ ) and C=C skeleton (1450  $cm^{-1}$ ) of the TC adsorbed on stevensite remain in the same frequencies as in the crystalline TC (not shown in the Fig. 10), in contrast to the band attributed to the amide vibration at 1524  $cm^{-1}$  in TC that shifted around 21  $cm^{-1}$  to a lower frequency (1503  $cm^{-1}$ ) adsorbed to stevensite, suggesting that the amide group played an important role on the TC adsorption and that cation exchange is not the only mechanism responsible for the adsorption. This shift to lower frequencies was interpreted by Porubcan et al. (1978) as coordination of TC with the exchangeable cations on the interlayer clay surface.

Further research will be focused on the study of complexation processes between the tetracycline and  $Mg^{2+}$  in the stevensite under specific experimental conditions relevant for retention of TC in waste water matrices (neutral pH and high ionic strength).

#### 4. Conclusions

Stevensite has been demonstrated to be an effective material for tetracycline adsorption since high adsorption capacity has been determined in batch experiments, which increases as pH increases from 2 to a range of 6–7.5, in contrast to previous natural clays studied as adsorbents. The zwitterionic species of tetracycline, dominant at pH 7, adsorb on stevensite in flow-through experiments by exceeding >3 times the cation exchange capacity of the clay. Therefore, complexation mechanisms with cations are assumed in addition to cation exchange in the interlayer of the smectite. Desorption of tetracycline by displacement with a  $Mg(NO_3)_2$  solution at acid pH is fast and recover the geofilter mixture to be used in an additional cycle of tetracycline adsorption. The results obtained in the present study are

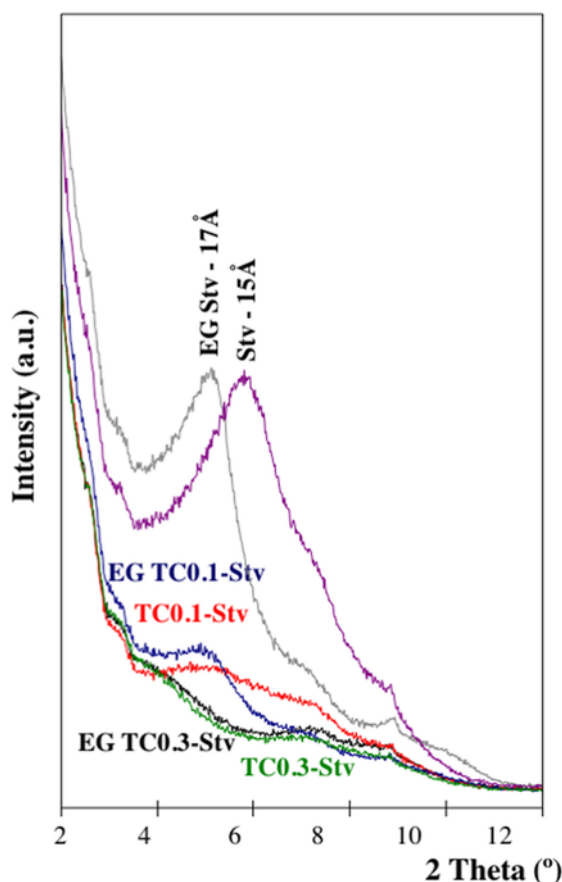


Fig. 9. XRD on oriented aggregate samples. Stv=stevensite; EG=ethylene-glycol; TC=tetracycline; 0.1 and 0.3 refers to the mass ratio per gram of stevensite.

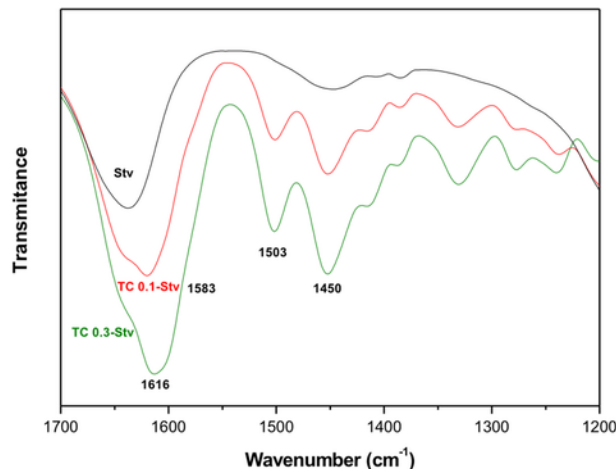


Fig. 10. IR spectra in the range 1700–1200  $cm^{-1}$  of the original stevensite (Stv; black) and TC-stevensite interaction in suspension tests at 0.1:1 (red) and 0.3:1 mass ratio (green). (For interpretation of the references to figures in this article legend, the reader is referred to the web version of this article.)

promising to implement a cost-effective design of tetracycline retention in waste water treatment plants.

Further investigation will be performed in order to assess the adsorption capacity of tetracycline by stevensite in complex wastewater matrices, and accurate clay characterization will be required to elucidate the adsorption mechanisms on stevensite.

## Acknowledgements

This work has been financially supported by the Spanish Ministry of Economy and Competitiveness through the AGL2016-78490-R project. Dr. García-Delgado thanks the Spanish Ministry of Economy and Competitiveness for his post-doctoral contract (JCFI-2015-23543).

## References

- Acosta, R., Fierro, V., Martínez de Yuso, A., Nabarlaz, D., Celzard, A., 2016. Tetracycline adsorption onto activated carbons produced by KOH activation of tyre pyrolysis char. *Chemosphere* 149, 168–176.
- Ahmed, M.B., Zhou, J.L., Ngo, H.H., Guo, W., 2015. Adsorptive removal of antibiotics from water and wastewater: progress and challenges. *Sci. Total Environ.* 532, 112–126.
- Antón-Herrero, R., García-Delgado, C., Alonso-Izquierdo, M., García-Rodríguez, G., Cuevas, J., Eymar, E., 2017. Comparative adsorption of tetracyclines on biochars and stevensite: looking for the most effective adsorbent. *Appl. Clay Sci.* (In press).
- Appelo, C.A.J., Postma, D., 2005. Flow and transport. In: Appelo, C.A.J., Postma, D. (Eds.), *Geochemistry, Groundwater and Pollution*. CRC Press, Taylor & Francis group, Amsterdam, the Netherlands, pp. 63–118.
- Aristilde, L., Marichal, C., Miché-Brendlé, J., Lanson, B., Charlet, L., 2010. Interactions of oxytetracycline with a smectite clay: a spectroscopic study with molecular simulations. *Environ. Sci. Technol.* 44, 7839–7845.
- Aristilde, L., Lanson, B., Miché-Brendlé, J., Marichal, C., Charlet, L., 2016. Enhanced interlayer trapping of a tetracycline antibiotic within montmorillonite layers in the presence of Ca and Mg. *J. Colloid Interface Sci.* 464, 153–159.
- Bolster, C.H., Hornberger, G.M., 2007. On the use of linearized Langmuir equations. *Soil Sci. Soc. Am. J.* 71, 1796–1806.
- Chang, P.-H., Jean, J.-S., Jiang, W.-T., Li, Z., 2009. Mechanism of tetracycline sorption on rectorite. *Colloids Surf. A Physicochem. Eng. Asp.* 339, 94–99.
- Chang, P.-H., Li, Z., Jiang, W.-T., Jean, J.-S., 2009. Adsorption and intercalation of tetracycline by swelling clay minerals. *Appl. Clay Sci.* 46, 27–36.
- Chang, P.-H., Li, Z., Jiang, W.-T., Kuo, C.-Y., Jean, J.-S., 2015. Adsorption of tetracycline on montmorillonite: influence of solution pH, temperature, and ionic strength. *Desalin. Water Treat.* 55, 1380–1392.
- Cheng, D., Liao, P., Yuan, S., 2016. Effects of ionic strength and cationic type on humic acid facilitated transport of tetracycline in porous media. *Chem. Eng. J.* 284, 389–394.
- Clive, D.L.J., 1968. Chemistry of tetracyclines. *Q. Rev. Chem. Soc.* 22, 435–456.
- Faust, G.T., Murata, K.J., 1953. Stevensite, redefined as a member of the montmorillonite group. *Am. Mineral.* 38, 973–987.
- Figuerola, R.A., Leonard, A., MacKay, A.A., 2004. Modeling tetracycline antibiotic sorption to clays. *Environ. Sci. Technol.* 38, 476–483.
- Güven, N., 1991. Smectites. In: *Hydrous Phyllosilicates (Exclusive of Micas)*. Washington D.C., Mineralogical Society of America, pp. 497–559.
- Homem, V., Santos, L., 2011. Degradation and removal methods of antibiotics from aqueous matrices – a review. *J. Environ. Manag.* 92, 2304–2347.
- Hou, J., Wang, C., Mao, D., Luo, Y., 2016. The occurrence and fate of tetracyclines in two pharmaceutical wastewater treatment plants of Northern China. *Environ. Sci. Pollut. Res.* 23, 1722–1731.
- Jin, L., Amaya-Mazo, X., Apel, M.E., Sankisa, S.S., Johnson, E., Zbyszynska, M.A., et al., 2007.  $\text{Ca}^{2+}$  and  $\text{Mg}^{2+}$  bind tetracycline with distinct stoichiometries and linked deprotonation. *Biophys. Chem.* 128, 185–196.
- Kang, H.-J., Lim, M.-Y., Kwon, J.-H., 2012. Effects of adsorption onto silica sand particles on the hydrolysis of tetracycline antibiotics. *J. Environ. Monit.* 14, 1853–1859.
- Kim, S., Eichhorn, P., Jensen, J.N., Weber, A.S., Aga, D.S., 2005. Removal of antibiotics in wastewater: effect of hydraulic and solid retention times on the fate of tetracycline in the activated sludge process. *Environ. Sci. Technol.* 39, 5816–5823.
- Kolpin, D.W., Furlong, E.T., Meyer, M.T., Thurman, E.M., Zaugg, S.D., Barber, L.B., et al., 2002. Pharmaceuticals, hormones, and other organic wastewater contaminants in U.S. streams, 1999–2000: a national reconnaissance. *Environ. Sci. Technol.* 36, 1202–1211.
- Li, D., Yang, M., Hu, J., Ren, L., Zhang, Y., Li, K., 2009. Determination and fate of oxytetracycline and related compounds in oxytetracycline production wastewater and the receiving river. *Environ. Toxicol. Chem.* 27, 80–86.
- Li, Z., Schulz, L., Ackley, C., Fenske, N., 2010. Adsorption of tetracycline on kaolinite with pH-dependent surface charges. *J. Colloid Interface Sci.* 351, 254–260.
- Madejová, J., Komadel, P., 2001. Baseline studies of the clay minerals society source clays: infrared methods. *Clay Clay Miner.* 49, 410–432.
- Mahamallik, P., Saha, S., Pal, A., 2015. Tetracycline degradation in aquatic environment by highly porous  $\text{MnO}_2$  nanosheet assembly. *Chem. Eng. J.* 276, 155–165.
- Meier, L.P., Kahr, G., 1999. Determination of the cation exchange capacity (CEC) of clay minerals using the complexes of copper(II) ion with triethylenetetramine and tetraethylenepentamine. *Clay Clay Miner.* 47, 386–388.
- Michael, I., Rizzo, L., McArdell, C.S., Manaia, C.M., Merlin, C., Schwartz, T., et al., 2013. Urban wastewater treatment plants as hotspots for the release of antibiotics in the environment: a review. *Water Res.* 47, 957–995.
- Miralles, N., Valderrama, C., Casas, I., Martínez, M., Florido, A., 2010. Cadmium and lead removal from aqueous solution by grape stalk wastes: modeling of a fixed-bed column. *J. Chem. Eng. Data* 55, 3548–3554.
- Moore, D.M., Reynolds, R.C., 1997. *X-Ray Diffraction and the Identification and Analysis of Clay Minerals*. Oxford University Press, London.
- Nir, S., Zadaka-Amir, D., Kartaginer, A., Gonen, Y., 2012. Simulation of adsorption and flow of pollutants in a column filter: application to micelle–montmorillonite mixtures with sand. *Appl. Clay Sci.* 67–68, 134–140.
- Othersen, O.G., Lanig, H., Clark, T., 2003. Systematic surface scan of the most favorable interaction sites of magnesium ions with tetracycline. *J. Med. Chem.* 46, 5571–5574.
- Parolo, M.E., Savini, M.C., Vallés, J.M., Baschini, M.T., Avena, M.J., 2008. Tetracycline adsorption on montmorillonite: pH and ionic strength effects. *Appl. Clay Sci.* 40, 179–186.
- Porubcan, L.S., Serna, C.J., White, J.L., Hem, S.L., 1978. Mechanism of adsorption of clindamycin and tetracycline by montmorillonite. *J. Pharm. Sci.* 67, 1081–1087.
- Ren, X., Zeng, G., Tang, L., Wang, J., Wan, J., Feng, H., et al., 2018. Effect of exogenous carbonaceous materials on the bioavailability of organic pollutants and their ecological risks. *Soil Biol. Biochem.* 116, 70–81.
- Ren, X., Zeng, G., Tang, L., Wang, J., Wan, J., Liu, Y., et al., 2018. Sorption, transport and biodegradation – an insight into bioavailability of persistent organic pollutants in soil. *Sci. Total Environ.* 610–611, 1154–1163.
- Toride, N., Leij, F.J., van Genuchten, M.T., 1995. The CXTFIT Code for Estimating Transport Parameters From Laboratory or Field Tracer Experiments. U. S. Salinity Laboratory, U. S. Department of Agriculture, Riverside, California, 137.
- Tran, N.H., Reinhard, M., Gin, K.Y.-H., 2018. Occurrence and fate of emerging contaminants in municipal wastewater treatment plants from different geographical regions—a review. *Water Res.* 133, 182–207.
- van Genuchten, M.T., Wagenet, R.J., 1989. Two-site/two-region models for pesticide transport and degradation: theoretical development and analytical solutions. *Soil Sci. Soc. Am. J.* 53, 1303–1310.
- van Genuchten, M.T., Šimunek, J., Leij, F.J., Toride, N., Šejna, M., 2012. STANMOD: model use, calibration, and validation. *Trans. ASABE* 55, 1353–1366.
- Wei, R., Ge, F., Huang, S., Chen, M., Wang, R., 2011. Occurrence of veterinary antibiotics in animal wastewater and surface water around farms in Jiangsu Province, China. *Chemosphere* 82, 1408–1414.
- Wessels, J.M., Ford, W.E., Szymczak, W., Schneider, S., 1998. The complexation of tetracycline and anhydrotetracycline with  $\text{Mg}^{2+}$  and  $\text{Ca}^{2+}$ : a spectroscopic study. *J. Phys. Chem. B* 102, 9323–9331.
- Yang, S., Carlson, K., 2003. Evolution of antibiotic occurrence in a river through pristine, urban and agricultural landscapes. *Water Res.* 37, 4645–4656.
- Zhao, Y., Gu, X., Gao, S., Geng, J., Wang, X., 2012. Adsorption of tetracycline (TC) onto montmorillonite: cations and humic acid effects. *Geoderma* 183–184, 12–18.
- Zhao, Y., Gu, X., Li, S., Han, R., Wang, G., 2015. Insights into tetracycline adsorption onto kaolinite and montmorillonite: experiments and modeling. *Environ. Sci. Pollut. Res.* 22, 17031–17040.